JOC Article

Gosteli−Claisen Rearrangement: DFT Study of Substituent−Rate Effects

Julia Rehbein* and Martin Hiersemann*

Fakultät Chemie, Technische Universität Dortmund, 44227 Dortmund, Germany

julia.rehbein@udo.edu; martin.hiersemann@udo.edu

Received March 25, 2009

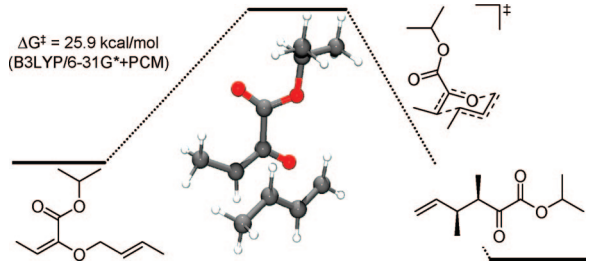

The uncatalyzed Gosteli−Claisen rearrangement of four double bond isomeric allyl vinyl ethers has been studied at the B3LYP/6-31G* and B3LYP/6-31G*+PCM levels of theory. The experimentally determined structure−reactivity relationship was successfully reproduced; the relative reactivity of the (*E*,*E*)-, (*E*,*Z*)-, (*Z*,*E*)-, and (*Z*,*Z*)-configured allyl vinyl ethers can be attributed to unfavorable interactions caused by pseudoaxial substituents within the chairlike transition-state structures. As expected, the isolated assessment of the calculated ground-state or transition-state stabilities is not suitable to explain the experimentally observed structure−reactivity relationship.

Introduction

The Gosteli−Claisen rearrangement is the [3,3]-sigmatropic rearrangement of an acyclic 2-alkoxycarbonyl-substituted allyl vinyl ether (Figure 1). The presence of the ester group at C2 of the allyl vinyl ether framework distinguishes the Gosteli−Claisen rearrangement from other, more popular Claisen rearrangement variants with respect to substrate synthesis, reactivity, and product structure. The first application of the Claisen rearrangement of a 2-alkoxycarbonyl-substituted allyl vinyl ether in synthesis was apparently reported by Gosteli in 1972 (Figure 2).[1] However, the chorismate mutase catalyzed Claisen rearrangement of chorismate to prephenate may be considered as the mother of all Claisen rearrangements of allyl vinyl ethers featuring a π-acceptor at the 2-position (Figure 3).[2]

The particular importance of the Gosteli−Claisen rearrangement is founded on the availability of chiral Lewis acid catalysts

FIGURE 1. Gosteli−Claisen rearrangement.

and organocatalysts for this rearrangement,[3] an opportunity that has been rarely realized for the more popular variants of the Claisen rearrangement.[4] In order to improve the existing catalyst systems, a detailed knowledge of the mechanism of the catalyzed and uncatalyzed Gosteli−Claisen rearrangement would certainly be beneficial. Kinetic studies on the Gosteli−Claisen rearrangement have been performed by Gajewski et al. in the context of the chorismate mutase research field.[5] It was established that the 2-CO_2Me group lowers the activation free energy (100 °C) by 3 kcal/mol compared to the parent allyl vinyl ether. Relying on experimentally determined rate constants and secondary

(1) Gosteli, J. *Helv. Chim. Acta* **1972**, *55*, 451–460.

(2) Gao, H.; Rao, N. Chorismate-Mutase-Catalyzed Claisen Rearrangement. In *The Claisen Rearrangement*; Hiersemann, M., Nubbemeyer, U., Eds.; Wiley-VCH: Weinheim 2007; pp 1−23.

(3) (a) Abraham, L.; Czerwonka, R.; Hiersemann, M. *Angew. Chem., Int. Ed.* **2001**, *40*, 4700–4703. (b) Abraham, L.; Körner, M.; Schwab, P.; Hiersemann, M. *Adv. Synth. Catal.* **2004**, *346*, 1281–1294. (c) Pollex, A.; Hiersemann, M. *Org. Lett.* **2005**, *7*, 5705–5708. (d) Körner, M.; Hiersemann, M. *Org. Lett.* **2007**, *9*, 4979–4982. (e) Uyeda, C.; Jacobsen, E. N. *J. Am. Chem. Soc.* **2008**, *130*, 9228–9229.

(4) For Claisen rearrangements of achiral aliphatic allyl vinyl ethers in the presence of catalytic amounts of a chiral catalyst, see: (a) Akiyama, K.; Mikami, K. *Tetrahedron Lett.* **2004**, *45*, 7217–7220. (b) Wender, P. A.; D'Angelo, N.; Elitzin, V. I.; Ernst, M.; Jackson-Ugueto, E. E.; Kowalski, J. A.; McKendry, S.; Rehfeuter, M.; Sun, R.; Voigtlaender, D. *Org. Lett.* **2007**, *9*, 1829–1832. (c) Linton, E. C.; Kozlowski, M. C. *J. Am. Chem. Soc.* **2008**, *130*, 16162–16163.

(5) Gajewski, J. J.; Jurayj, J.; Kimbrough, D. R.; Gande, M. E.; Ganem, B.; Carpenter, B. K. *J. Am. Chem. Soc.* **1987**, *109*, 1170–1186.

10.1021/jo900635k CCC: $40.75
Published on Web 05/12/2009

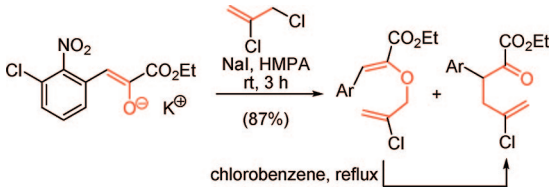

FIGURE 2. First application of a Gosteli−Claisen rearrangement in synthesis.

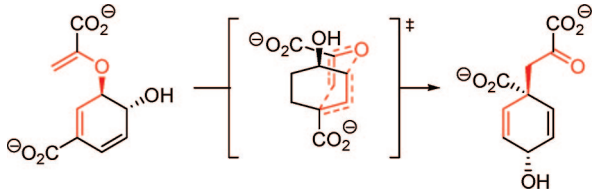

FIGURE 3. Chorismate−prephenate rearrangement.

deuterium kinetic isotope effects, Gajewski concluded that "an ester group at C-2 of an acyclic allyl vinyl ether accelerates the rate of the Claisen rearrangement by promoting stronger bond making in the transition state".[6] The first computational effort on the Gosteli−Claisen rearrangement was aimed at the explanation of the so-called "aqueous acceleration",[7] a rate-accelerating solvent effect observed for the Gosteli−Claisen rearrangement in a 3:1 mixture of methanol and water compared to cyclohexane.[5] The study inter alia revealed that the s-*cis* and s-*trans* conformational isomers of the ground and transition-states of the 2-CO_2Me-substituted allyl vinyl ether are close in energy. Therefore, a Boltzmann weighting of the energies of the s-*cis* and s-*trans* conformers was applied. Wiest and Houk have studied the Claisen rearrangement of the 2-CO_2H-substituted allyl vinyl ether computationally at the B3LYP/6-31G* level of theory.[8] With respect to the rate-accelerating effect of the carboxyl group, it was concluded that "the substantial activation energy lowering arises from the stabilization of the developing partial charge on the enolate group in the transition state".[9] Further computational studies have been reported by Strassner et al.[10] and Balta et al.[11] in the context of the organo or Lewis acid catalyzed Gosteli−Claisen rearrangement; however, these studies consider neither s-*cis*/s-*trans* conformational issues nor the influence of the double bond configuration on the free energy of activation.

We have recently reported the results of a study aimed at the quantification of substituent rate effects of the Gosteli−Claisen rearrangement.[12] In this context, we experimentally determined the rate constants and free energies of activation ($\Delta G^{\ddagger}$) for the rearrangement of the allyl vinyl ethers **1a**−**d** (Figure 4); as

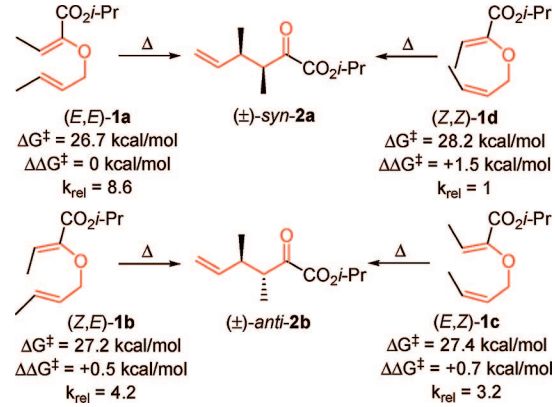

FIGURE 4. Experimentally determined (1,2-dichloroethane, 80 °C) substituent−rate effect of methyl groups on the Gosteli−Claisen rearrangement.

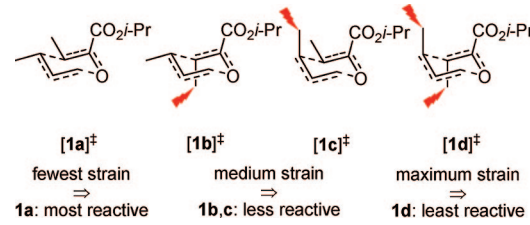

FIGURE 5. Rating the relative reactivity of **1a**−**d** based on unfavorable transannular interactions within the transition-state structures [**1a**−**d**]‡. Tick marks signify the strain-causing methyl group(s).

expected, we found that the reactivity of **1a**−**d** depends on the configuration of the two stereogenic double bonds.

To account for the experimental substrate−reactivity relationship, we used a qualitative model[13] that considers only the number of pseudoaxial methyl groups causing unfavorable transannular interactions (strain) in the idealized transition-state structures [**1a**−**d**]‡ to estimate the relative reactivity of the corresponding allyl vinyl ethers (Figure 5). The resulting qualitative reactivity order is consistent with the experiment, which is particularly impressive given the small experimental $\Delta\Delta G^{\ddagger}$ values.

To verify the orientating paradigm−relative transition-state strain as determinant for relative reactivity−of the employed qualitative strain−reactivity model, we have computationally studied the Gosteli−Claisen rearrangement of the four constitutionally identical, diastereomeric allyl vinyl ethers **1a**−**d** at the B3LYP/6-31G* and B3LYP/6-31G*+PCM level of theory.

Computational Methods

Hybrid density functional theory[14] calculations were performed with the Gaussian03[15] suite of programs. Harmonic vibrational frequency calculations confirmed stationary points either as minima (number of imaginary frequencies, NIMAG = 0) or as transition-states (NIMAG = 1).[16] For each transition-state, IRC[17] calculations were performed in both directions to locate the nearest stationary points; the resulting structures were subjected to geometry optimization and frequency calculations; the computed compounds are denoted as sc/st-**1a**−**d*** or sc-**2a**−**d***. Approximate free energies

(6) For ^{14}C kinetic isotope effects for the Gosteli−Claisen rearrangement of the 2-methoxycarbonyl-substitued allyl vinyl ether, see: Kupczyk-Subotkowska, L.; Saunders, W. H.; Shine, H. J.; Subotkowski, W. *J. Am. Chem. Soc.* **1994**, *116*, 7088–7093.

(7) Cramer, C. J.; Truhlar, D. G. *J. Am. Chem. Soc.* **1992**, *114*, 8794–8799.

(8) Wiest, O.; Houk, K. N. *J. Am. Chem. Soc.* **1995**, *117*, 11628–11639.

(9) The Claisen rearrangement of the 2-cyano-substituted allyl vinyl ether was also studied computationally. It was stated that the rate-accelerating effect of a 2-CN group is the consequence of an intrinsic transition-state stabilizing effect and that "this arises from the stabilization of the developing partial negative charge on the enolate group in the transition state". See: Aviyente, V.; Yoo, H. Y.; Houk, K. N. *J. Org. Chem.* **1997**, *62*, 6121–6128.

(10) Kirsten, M.; Rehbein, J.; Hiersemann, M.; Strassner, T. *J. Org. Chem.* **2007**, *72*, 4001–4011.

(11) Öztürk, C.; Balta, B.; Aviyente, V.; Vincent, M. A.; Hillier, I. H. *J. Org. Chem.* **2008**, *73*, 4800–4809.

(12) Rehbein, J.; Leick, S.; Hiersemann, M. *J. Org. Chem.* **2009**, *74*, 1531–1540.

(13) (a) Vittorelli, P.; Winkler, T.; Hansen, H.-J.; Schmid, H. *Helv. Chim. Acta* **1968**, *51*, 1457–1461. (b) Perrin, C. L.; Faulkner, D. J. *Tetrahedron Lett.* **1969**, *10*, 2783–2786. (c) Hansen, H.-J.; Schmid, H. *Tetrahedron* **1974**, *30*, 1959–1969.

(14) Kohn, W.; Becke, A. D.; Parr, R. G. *J. Phys. Chem.* **1996**, *100*, 12974–12980.

were obtained by thermochemical analysis of the frequency calculation, using the thermal correction to the Gibbs free energy as reported by Gaussian03. This takes into account zero-point effects, thermal enthalpy corrections, and entropy. Frequencies remained unscaled. For the determination of atomic charges, Mulliken population analysis (MPA)[18] and natural population analysis (NPA)[19,20] were applied. The NBO[21] approach was used to analyze delocalization effects by means of NBO version 3.0 as implemented in Gaussian03. Xyz-matrices were written with the freeware program Gabedit. Geometric data were determined with Molden for Linux. Boltzmann-averaged free energies were calculated according to $\Delta G_{\varnothing} = (f\Delta G_{s\text{-}cis} + \Delta G_{s\text{-}trans})/(1 + f)$ with $f = N_{s\text{-}cis}/N_{s\text{-}trans} = \exp(-[\Delta G_{s\text{-}cis} - \Delta G_{s\text{-}trans}]/RT)$. The order of the breaking and the forming σ-bonds in the transition-state structures were calculated using the Pauling relation $n_p/n_0 = \exp[(d_0 - d)/c]$ with $n_0 = 1$ and $c = 0.6$ as described by Singleton.[22] Condensed-phase effects were approximated by treating the solvent as a polarizable continuum medium. The solvent effect of 1,2-dichloroethane was calculated using a polarized continuum model (IEF-PCM[23]) as implemented in Gaussian 03; the condensed-phase structures were fully optimized and subjected to frequency calculations at the B3LYP/6-31G*+PCM level of theory using the implemented parameters for 1,2-dichloroethane.

Although various computational methods have been utilized to study the thermal Claisen rearrangement of aliphatic allyl vinyl ethers in the gas phase,[24] application of the B3LYP[25] functional in combination with the 6-31G(d)[26] basis set is currently the best compromise[10,27] between cost and accuracy. With respect to the Claisen rearrangement of the unsubstituted parent allyl vinyl ether, MP4/6-31G*//RHF/6-31G* and B3LYP/6-31G* calculations provide activation barriers that correlate well with the experimental values.[28] It was also shown that activation parameters from B3LYP/6-31G* calculations for the parent allyl vinyl ether are in better agreement with the experimental data compared to RHF/6-31G* and CASSCF/6-31G*.[29,30] For the Claisen rearrangement of the parent allyl vinyl ether, DFT calculations using the B3LYP functional and the 6-31G*, 6-31G**, and 6-311+G** functional predicted comparable free energies of activation and also provided very good estimates of the transition-state structure judging from the comparison of experimental and calculated kinetic isotope effects.[30,31] A comparison of computationally predicted activation parameters at various levels of theory with the experimental values for the parent allyl vinyl ether led Menger et al. to the conclusion that the B3LYP method is superior to BLYP, SVWN, and MP2.[32] Singleton concluded that the nature of the transition-state of the Claisen rearrangement of the parent allyl vinyl ether is somewhere between the structures predicted by B3LYP/6-31G* and MP2/6-31G* and that the transition-structure geometry is best described by the MP4/6-31G* structure.[22] For the Claisen rearrangement of the parent allyl vinyl ether in di-*n*-butyl ether, Hillier has demonstrated that the PCM approximation is in good agreement with the experiment.[33]

Results and Discussion

Free Energy Profile for the Gosteli−Claisen Rearrangement. We started our study by calculating the free energy profiles for the uncatalyzed Gosteli−Claisen rearrangement of **1a**−**d**. As pointed out by Cramer and Truhlar,[7] the theoretical study of the Gosteli−Claisen rearrangement has to consider the involvement of two distinguished conformers with respect to the dihedral orientation of the vinyl ether double bond and the carbonyl double bond. Relying on the resonance concept, it is reasonable to assume that the "planar" s-*cis* and s-*trans* conformers should be energetically most favorable. Therefore, we have restricted the conformational space by modeling the s-*cis* (sc) and s-*trans* (st) pathways for the Gosteli−Claisen rearrangement. As illustrated for **1a** in Scheme 1, the s-*cis* pathway proceeds from the stretched s-*cis* conformer sc-**1a** via the bend "reactive conformer" sc-**1a*** to the chairlike transition-state structure [sc-**1a**]‡ and provides the bend s-*trans* conformer st-**2a*** of the α-keto ester. The s-*trans* pathway proceeds from st-**1a** via st-**1a*** and [st-**1a**]‡ to afford the α-keto ester conformer sc-**2a***. The corresponding free energy profiles for **1a**−**d** were calculated at the B3LYP/6-31G* and the B3LYP/6-31G*+PCM(solvent = 1,2-dichloroethane) levels of theory. Experimentally, 1,2-dichloroethane was used as solvent for the

(15) Frisch, M. J.; Trucks, G. W.; Schlegel, H. B.; Scuseria, G. E.; Robb, M. A.; Cheeseman, J. R. ; Montgomery, J. A., Jr.; Vreven, T.; Kudin, K. N. ; Burant, J. C.; Millam, J. M.; Iyengar, S. S.; Tomasi, J.; Barone, V.; Mennucci, B.; Cossi, M.; Scalmani, G.; Rega, N.; Petersson, G. A.; Nakatsuji, H.; Hada, M.; Ehara, M.; Toyota, K.; Fukuda, R.; Hasegawa, J.; Ishida, M.; Nakajima, T.; Honda, Y.; Kitao, O.; Nakai, H.; Klene, M.; Li, X.; Knox, J. E.; Hratchian, H. P.; Cross, J. B.; Bakken, V.; Adamo, C.; Jaramillo, J.; Gomperts, R.; Stratmann, R. E.; Yazyev, O.; Austin, A. J.; Cammi, R.; Pomelli, C.; Ochterski, J. W.; Ayala, P. Y.; Morokuma, K.; Voth, G. A.; Salvador, P.; Dannenberg, J. J.; Zakrzewski, V. G.; Dapprich, S.; Daniels, A. D.; Strain, M. C.; Farkas, O.; Malick, D. K.; Rabuck, A. D.; Raghavachari, K.; Foresman, J. B.; Ortiz, J. V.; Cui, Q.; Baboul, A. G.; Clifford, S.; Cioslowski, J.; Stefanov, B. B.; Liu, G.; Liashenko, A.; Piskorz, P.; Komaromi, I.; Martin, R. L.; Fox, D. J.; Keith, T.; Al-Laham, M. A.; Peng, C. Y.; Nanayakkara, A.; Challacombe, M.; Gill, P. M. W.; Johnson, B.; Chen, W.; Wong, M. W.; Gonzalez, C.; Pople, J. A. *Gaussian03, Rev. D 02*; Gaussian, Inc.: Wallingford, CT, 2004.

(16) McIver, J. W.; Komornicki, A. K. *J. Am. Chem. Soc.* **1972**, *94*, 2625–2633.

(17) (a) Gonzalez, C.; Schlegel, H. B. *J. Chem. Phys.* **1989**, *90*, 2154–2161. (b) Gonzalez, C.; Schlegel, H. B. *J. Phys. Chem.* **1990**, *94*, 5523–5527.

(18) Mulliken, R. S. *J. Chem. Phys.* **1955**, *23*, 1833–1840.

(19) Reed, E. A.; Weinstock, R. B.; Weinhold, F. *J. Chem. Phys.* **1988**, *83*, 735–746.

(20) (a) Wiberg, K. B.; Rablem, P. R. *J. Comput. Chem.* **1993**, *14*, 1504–1518. (b) McAllister, M. A.; Tidwell, T. T. *J. Org. Chem.* **1994**, *59*, 4506–4515.

(21) (a) Foster, J. P.; Weinhold, F. *J. Am. Chem. Soc.* **1980**, *102*, 7211–7218. (b) Reed, A. E.; Curtiss, L. A.; Weinhold, F. *Chem. Rev.* **1988**, *88*, 899–926.

(22) Meyer, M. P.; DelMonte, A. J.; Singleton, D. A. *J. Am. Chem. Soc.* **1999**, *121*, 10865–10874.

(23) (a) Cancès, E.; Mennucci, B.; Tomasi, J. *J. Chem. Phys.* **1997**, *107*, 3032–3041. (b) Tomasi, J.; Mennucci, B.; Cammi, R. *Chem. Rev.* **2005**, *105*, 2999–3093. (c) Klamt, A.; Mennucci, B.; Tomasi, J.; Barone, V.; Curutchet, C.; Orozco, M.; Luque, F. J. *Acc. Chem. Res.* **2009**, *42*, 489–492.

(24) (a) Burrows, C.; Carpenter, B. K. *J. Am. Chem. Soc.* **1981**, *103*, 6984–6986. (b) Dewar, M. J. S.; Healy, E. F. *J. Am. Chem. Soc.* **1984**, *106*, 7127–7131. (c) Vance, R. L.; Rondan, N. G.; Houk, K. N.; Jensen, F.; Borden, W. T.; Komornicki, A.; Wimmer, E. *J. Am. Chem. Soc.* **1988**, *110*, 2314–2315. (d) Dewar, M. J. S.; Jie, C. *J. Am. Chem. Soc.* **1989**, *111*, 511–519. (e) Severance, D. L.; Jorgensen, W. L. *J. Am. Chem. Soc.* **1992**, *114*, 10966–10968. (f) Cramer, C. J.; Truhlar, D. G. *J. Am. Chem. Soc.* **1992**, *114*, 8794–8799. (g) Davidson, M. M.; Hillier, I. H.; Hall, R. J.; Burton, N. A. *J. Am. Chem. Soc.* **1994**, *116*, 9294–9297. (h) Yoo, H. Y.; Houk, K. N. *J. Am. Chem. Soc.* **1994**, *116*, 12047–12048. (i) Sehgal, A.; Shao, L.; Gao, J. *J. Am. Chem. Soc.* **1995**, *117*, 11337–11340. (j) Gao, J. *J. Am. Chem. Soc.* **1994**, *116*, 1563–1564. (k) Davidson, M. M.; Hillier, I. H. *J. Phys. Chem.* **1995**, *99*, 6748–6751. (l) Khaledy, M. M.; Kalani, M. Y. S.; Khuong, K. S.; Houk, K. N.; Aviyente, V.; Neier, R.; Soldermann, N.; Velker, J. *J. Org. Chem.* **2003**, *68*, 572–577. (n) Plazuk, D.; Warkentin, J.; Werstiuk, N. H. *Tetrahedron* **2005**, *61*, 5788–5796. (o) Ozturk, C.; Aviyente, V.; Houk, K. N. *J. Org. Chem.* **2005**, *70*, 7028–7034. (p) Zhang, Y.-D.; Ren, W.-W.; Lan, Y.; Xiao, Q.; Wang, K.; Xu, J.; Chen, J.-H.; Yang, Z. *Org. Lett.* **2008**, *10*, 665–668.

(25) (a) Becke, A. D. *Phys. Rev. A* **1988**, *38*, 3098–3100. (b) Lee, C.; Yang, W.; Parr, R. G. *J. Phys. Rev.* **1988**, *37*, 785–789. (c) Becke, A. D. *J. Chem. Phys.* **1993**, *98*, 5648–5652. (d) Stephens, P. J.; Devlin, F. J.; Chabalowski, C. F.; Frisch, M. J. *J. Phys. Chem.* **1994**, *98*, 11623–11627.

(26) (a) Hehre, W. J.; Ditchfield, R.; Pople, J. A. *J. Chem. Phys.* **1972**, *56*, 2257–2261. (b) Hariharan, P. C.; Pople, J. A. *Theor. Chim. Acta* **1973**, *28*, 213–222.

(27) Aviyente, V.; Houk, K. N. *J. Phys. Chem. A* **2001**, *105*, 383–391.

(28) Yamabe, S.; Okumoto, S.; Hayashi, T. *J. Org. Chem.* **1996**, *61*, 6218–6226.

(29) Aviyente, V.; Yoo, H. Y.; Houk, K. N. *J. Org. Chem.* **1997**, *62*, 6121–6128.

(30) Wiest, O.; Black, K. A.; Houk, K. N. *J. Am. Chem. Soc.* **1994**, *116*, 10336–10337.

(31) Hu, H.; Kobrak, M. N.; Xu, C.; Hammes-Schiffer, S. *J. Phys. Chem. A* **2000**, *104*, 8058–8066.

(32) Khanjin, N. A.; Snyder, J. P.; Menger, F. M. *J. Am. Chem. Soc.* **1999**, *121*, 11831–11846.

(33) Davidson, M. M.; Hillier, I. H.; Hall, R. J.; Burton, N. A. *J. Am. Chem. Soc.* **1994**, *116*, 9294–9297.

SCHEME 1. s-*cis* and s-*trans* Pathways for the Gosteli−claisen Rearrangement of the Allyl Vinyl Ether 1a[a]

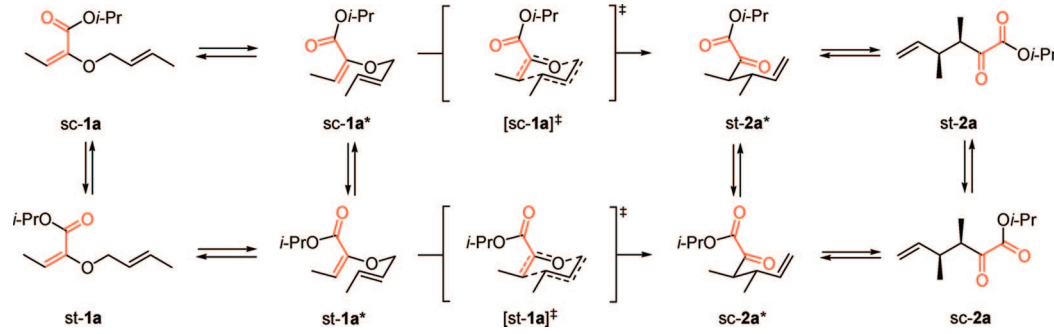

[a] sc = s-*cis*, st = s-*trans*.

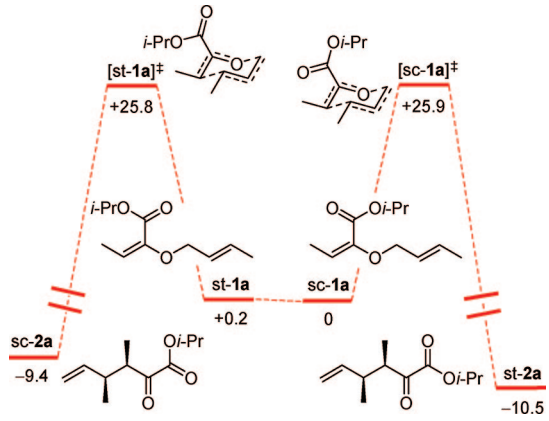

FIGURE 6. Free energy profile for the Gosteli−Claisen rearrangement of **1a** at the B3LYP/6-31G*+PCM(solvent = 1,2-dichloroethane) level of theory (kcal/mol at 298.15 K).

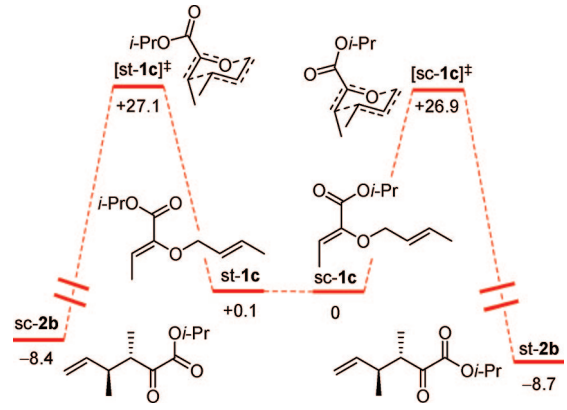

FIGURE 8. Free energy profile for the Gosteli−Claisen rearrangement of **1c** at the B3LYP/6-31G*+PCM(solvent = 1,2-dichloroethane) level of theory (kcal/mol at 298.15 K).

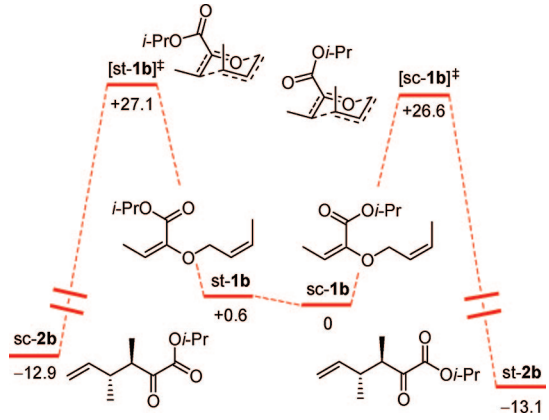

FIGURE 7. Free energy profile for the Gosteli−Claisen rearrangement of **1b** at the B3LYP/6-31G*+PCM(solvent = 1,2-dichloroethane) level of theory (kcal/mol at 298.15 K).

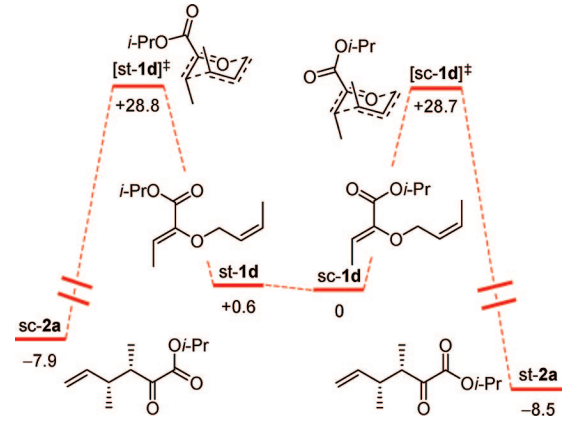

FIGURE 9. Free energy profile for the Gosteli−Claisen rearrangement of **1d** at the B3LYP/6-31G*+PCM(solvent = 1,2-dichloroethane) level of theory (kcal/mol at 298.15 K).

uncatalyzed Gosteli−Claisen rearrangement of **1a**−**d**.[12] The B3LYP/6-31G* energies are included in Supporting Information. All of the depicted conformers and transition-states have been verified as stationary points by harmonic vibrational frequency calculations. Furthermore, IRC calculations were performed to trace the reaction pathway from the transition-state [st-/sc-**1**]‡ to the allyl vinyl ether conformer st-/sc-**1*** and to the α-keto ester conformer st-/sc-**2***. For the sake of clarity, however, the bend conformers **1a**−**d*** and **2a**−**d*** are omitted from the discussion but are included in Supporting Information.

Our computations predict similar free energy profiles for the Gosteli−Claisen rearrangement of **1a**−**d** (Figures 6, 7, 8, and 9); in particular, the calculated free energies of activation for the s-*cis* and s-*trans* pathway via a chairlike transition-state structure are very close. The alternative boatlike transition-state structures were localized as stationary points at the B3LYP/6-31G* level of theory; depending on the double bond configuration, they are less favorable by >3 kcal/mol, a value that is in agreement with the experimentally determined[12] diastereoselectivity of >95/5 and the computational results of Balta et al.[11] Furthermore, our computations predict that the rearrangement is exergonic, which is in accordance with the experimentally observed complete conversion. In compliance with previous computational studies,[34] the s-*cis* conformer of the α-keto ester **2a**−**d** is less stable than the s-*trans* conformer st-**2a**−**d**. This has been attributed to the more favorable arrangement of the local

(34) Ferri, D.; Bürgi, T.; Baiker, A. *J. Chem. Soc., Perkin Trans. 2* **2000**, 221–227.

TABLE 1. Comparison of Boltzmann Averaged B3LYP/6-31G*+PCM(solvent = 1,2-dichloroethane) and Experimentally Determined $\Delta G^{\ddagger}$ (kcal/mol) at 353.15 and 298.15 K (Extrapolated)

		$\Delta G^{\ddagger}$		
entry	compd	expt (80 °C)[a]	expt (25 °C)[b]	calcd[c]
1	**1a**	26.7	25.0	25.8
2	**1b**	27.4	25.9	26.7
3	**1c**	27.2	26.1	26.9
4	**1d**	28.2	27.6	28.5

[a] Experimentally determined in 1,2-dichloroethane (kcal/mol at 353.15 K). [b] Extrapolated to 298.15 K according to $\Delta G^{\ddagger} = \Delta H^{\ddagger} - T\Delta S^{\ddagger}$ in kcal/mol. [c] B3LYP/6-31G*+PCM(solvent = 1,2-dichloroethane) (kcal/mol at 298.15 K).

TABLE 2. B3LYP/6-31G*+PCM(solvent = 1,2-dichloroethane) Relative Free Energy (G^{ts}_{rel}) at 298.15 K, Bond Lengths, and Order of the Breaking ($d_{O1-C1'}$) and the Forming Bond ($d_{C3-C3'}$), Dihedral Angles ω, and Dipole Moments μ for Transition-State Structures [sc-1a−d]‡

entry	compd	double bond config	G^{ts}_{rel} [kcal/mol]	$d_{O1-C1'}$ [Å] (n)[a]	$d_{C3-C3'}$ [Å] (n)[b]	ω[c] [deg]	μ [D]
1	[sc-**1a**]‡	(*E*,*E*)	0	2.058 (0.35)	2.369 (0.26)	−32	3.8
2	[sc-**1b**]‡	(*E*,*Z*)	+1.78	2.022 (0.38)	2.371 (0.26)	−31	3.7
3	[sc-**1c**]‡	(*Z*,*E*)	−1.96	2.062 (0.36)	2.409 (0.24)	−12	3.4
4	[sc-**1d**]‡	(*Z*,*Z*)	+1.13	2.044 (0.37)	2.426 (0.23)	−17	3.3

[a] Bond order n in % calculated according to Pauling: $n = n_o \times \exp[(d_{ave} - d_{ts})/0.6] \times 100\%$; $n_o = 1$. [b] Bond order n in % calculated according to Pauling: $n = n_o \times \exp[(d_{\alpha\text{-ke}} - d_{ts})/0.6] \times 100\%$; $n_o = 1$. [c] As defined in Figure 10.

dipole moments of the two carbonyl groups in s-*trans* conformers of α-keto esters.[34]

Calculated and Experimental Free Energies of Activation. Since the computed free energies for the reactants (st/sc-**1a−d**) and transition-states (st/sc-**1a−d**) of the s-*cis* and s-*trans* pathway are very close, Boltzmann averaged free energies of activation were calculated (Table 1). A comparison of the experimentally determined and Botzmann averaged B3LYP/6-31G*+PCM free energies of activation reveals a good agreement between theory and experiment. The condensed-phase computations overestimate the barrier for the rearrangement by 0.8 kcal/mol compared to the extrapolated experimental values at 25°C.

Transition-State Structure and Stability. The consistency of the experimental and the calculated $\Delta G^{\ddagger}$ values encouraged us to continue with our objective to support the qualitative strain-reactivity model by calculation. For this purpose, we first compared the relative free energies of the computated transition-states [sc-**1a−d**]‡ for the Gosteli−Claisen rearrangement (Table 2). Here, we will consider only the s-*cis* pathway, however, an analogous discussion for the s-*trans* pathway leads to identical conclusions.[35]

Regardless of the s-*cis* or s-*trans* conformation, our calculations predict that the relative free energies of [**1a−d**]‡ are inconsistent with the experimentally determined order of reactivity (Table 2, the values for the s-*trans* pathway are given in Supporting Information). The results of our calculations are illustrated for the s-*cis* pathway in Figure 10 using [sc-**1a**]‡ as point of reference. Surprisingly, [sc-**1c**]‡ is more stable than [sc-**1a**]‡ by 2 kcal/mol despite the fact that [sc-**1c**]‡ contains a pseudoaxial methyl group. Furthermore, [sc-**1d**]‡, despite featuring two pseudoaxial methyl groups, is more stable than [sc-**1b**]‡ by 0.65 kcal/mol. It is apparent from these results that the relative stability of the four transition-state structures [sc-**1a−d**]‡ is not determined *only* by the number and position of pseudoaxial substituents and that the relative transition-state stability cannot be used to assess the relative reactivity of the allyl vinyl ethers sc-**1a−d**. The question immediately emerges regarding which other geometric properties of the transition-state structures [sc-**1a−d**]‡ bias their relative stability. In order to answer that question, we next considered the critical geometric and electronic properties of [sc-**1a−d**]‡ that are summarized in Table 3. At first, the inspection of the lengths and the bond order n of the breaking ($d_{O1-C1'}$) and the forming bond ($d_{C3-C3'}$) revealed that the Gosteli−Claisen rearrangement of sc-**1a−d** is characterized by an asynchronous bond reorganization process; the breaking O1/C1′ bond is elongated by about 65%, whereas the nascent C3/C3′ bond is only established by about 25%. Because the asynchronity of the bond reorganization process is virtually identical for [sc-**1a−d**]‡, the relative transition-state stability can not be related to the looseness of the transition-state structures. Next, we compared the molecular dipole moment of [sc-**1a−d**]‡ that can be attributed to the interfragment charge separation; here again, almost identical dipole moments were calculated for [sc-**1a−d**]‡. Finally, assuming that the rate-accelerating effect of the ester group at the 2-position of the allyl vinyl ether core is intrinsic in nature and a consequence of a stabilizing conjugative interaction of the ester carbonyl group with the highly delocalized π-electron density of the transition-state structure, an increasing deviation of the dihedral angle ω from the ideal value of 0° should be destabilizing. In fact, the consideration of the dihedral angle ω assists in understanding the unexpected relative stability of [sc-**1a−d**]‡. In detail, [sc-**1a**]‡ ($\omega = -32°$) is less stable than [sc-**1c**]‡ ($\omega = -12°$) because of the more significant dihedral distortion that overcompensates for the destabilization of [sc-**1c**]‡ by the pseudoaxial methyl group at C3. The transition-state structures [sc-**1a**]‡ ($\omega = -32°$) is 1.8 kcal/mol more stable than [sc-**1b**]‡ ($\omega = -31°$), which is destabilized by the pseudoaxial methyl group at C3′. The comparison of [sc-**1b**]‡ with [sc-**1d**]‡ provides more insight into the subtle structure−stability interplay. Despite the fact that [sc-**1d**]‡ ($\omega = -17°$) features two pseudoaxial methyl groups and [sc-**1b**]‡ ($\omega = -31°$) only one, [sc-**1d**]‡ is more stable by 0.65 kcal/mol, obviously the consequence of the more favorable dihedral angle.

Ground-State Stability and Transition-State Strain. Because the relative transition-state stability (ΔG^{ts}_{rel}) alone does not reflect the experimentally observed relative reactivity (k_{rel}) according to Figure 5, we continued our study by evaluating the relative free energies (G^{ave}_{rel}) of the allyl vinyl ethers sc-**1a−d** and the change in G^{ave}_{rel} (ΔG_{rel}) on the way to the transition-states [sc-**1a−d**]‡ (Table 3, Figure 10, the values for the s-*trans* pathway are given in Supporting Information).

G^{ave}_{rel} for *sc*-**1a−d** varies within a range of 4 kcal/mol and is determined by the double bond configuration. With respect to the vinyl ether double bond, the *Z*-configuration is more favorable because the carbonyl group adopts a s-*cis* conformation closer to coplanarity: (*Z*,*E*)-sc-**1c** ($\omega = -9°$) is more stable than (*E*,*E*)-sc-**1a** ($\omega = +18°$) by 2.9 kcal/mol and (*Z*,*Z*)-sc-**1d** ($\omega = -8°$) is more stable than (*Z*,*Z*)-sc-**1b** ($\omega = +18°$) by 2.8 kcal/mol. As expected, an *E*-configured allyl ether double bond is more favorable than a *Z*-configured: (*E*,*E*)-sc-**1a** ($\omega = +18°$) is more stable than (*E*,*Z*)-sc-**1b** ($\omega = +18°$) by 1.1 kcal/mol and (*Z*,*E*)-sc-**1c** ($\omega = -9°$) is more stable than (*Z*,*Z*)-sc-**1d** ($\omega = -8°$) by 1.2 kcal/mol. By going from the ground to the transition-state, the stability of [sc-**1b−d**] declines relative to [sc-**1a**]; this observation can be attributed to an inherent strain within [sc-**1b−d**]‡ that is minimized in [sc-**1a**]‡. In detail, (*Z*,*E*)-sc-**1c** is more stable than (*E*,*E*)-sc-**1a** by 2.92 kcal/mol, but this gap is diminished by 0.96 to 1.96 kcal/mol if one compares the corresponding transition states [sc-**1a**]‡ and [sc-**1c**]‡. (*E*,*Z*)-sc-**1b** is less stable than (*E*,*E*)-sc-**1a** by 1.09 kcal/mol, and this gap is increased by 0.68 to 1.78 kcal/mol if the corresponding transition states [sc-**1a**]‡ and [sc-**1c**]‡ are compared. The transition-state structures [sc-**1b**]‡ and [sc-**1c**]‡ both feature a pseudoaxial methyl group and are therefore destabilized by transannular interactions relative to [sc-**1a**]‡. Finally, (*Z*,*Z*)-sc-**1d** is more stable

(35) See Supporting Information.

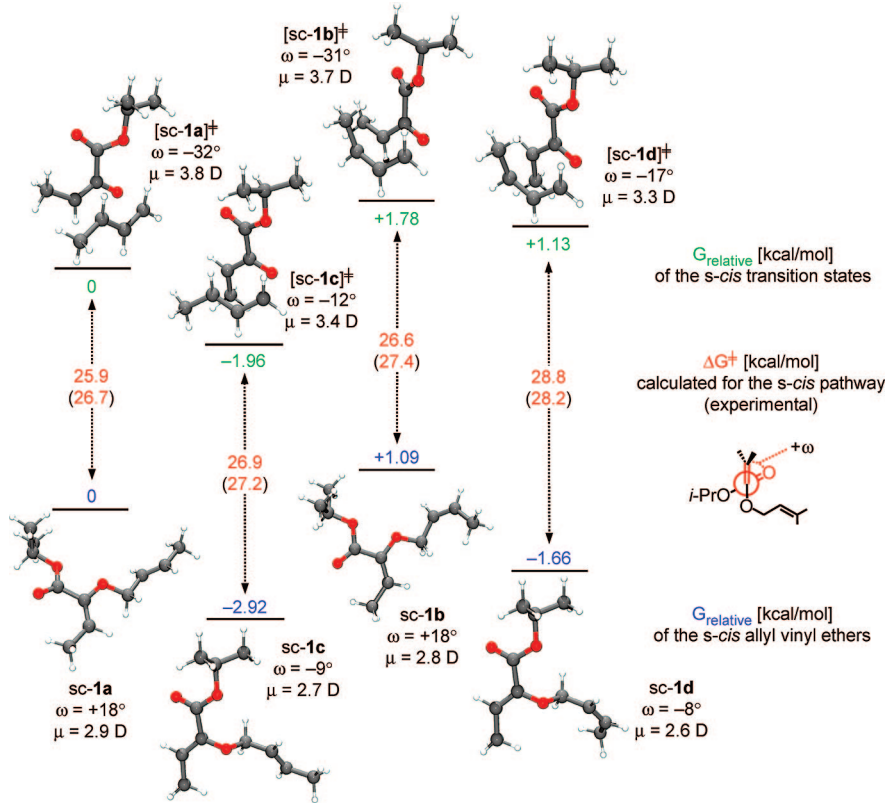

FIGURE 10. Relative free energies G_{rel} for sc-**1a**−**d**, [sc-**1a**−**d**]‡, and the calculated (experimental) free energies of activation $\Delta G^{‡}$ at the B3LYP/6-31G*+PCM(solvent = 1,2-dichloroethane) level of theory in kcal/mol at 298.15 K. Definition of the dihedral angle ω.

TABLE 3. B3LYP/6-31G*+PCM(solvent = 1,2-dichloroethane) Relative Free Energies (G^{ave}_{rel}), Bond Lengths of the Breaking ($d_{O1-C1'}$) Bond, Dihedral Angles ω, and Dipole Moments μ of Allyl Vinyl Ethers sc-1a−d at 298.15 K

entry	comp	config	G^{ave}_{rel} [kcal/mol]	ΔG_{rel}[a] [kcal/mol]	$d_{O1-C1'}$ [Å]	ω[b] [deg]	μ [D]
1	sc-**1a**	(*E*,*E*)	0	0	1.435	+18	2.9
2	sc-**1b**	(*E*,*Z*)	+1.09	+0.69	1.434	+18	2.8
3	sc-**1c**	(*Z*,*E*)	−2.92	+0.96	1.450	−9	2.7
4	sc-**1d**	(*Z*,*Z*)	−1.66	+2.79	1.449	−8	2.6

[a] Loss of stability on the way to the transition-state, relative to sc-**1a**. Calculated according to $|\Delta G_{rel}| = |G^{ave}_{rel}| - |G^{ts}_{rel}|$ for sc-**1b**,**c** and $|\Delta G_{rel}| = |G^{ave}_{rel}| + |G^{ts}_{rel}|$ for sc-**1d**. [b] As defined in Figure 10.

than (*E*,*E*)-sc-**1a** by 1.66 kcal/mol, but [sc-**1d**]‡ is less stable than [sc-**1a**]‡ by 1.13 kcal/mol. This huge drop of stability can be attributed to the presence of two pseudoaxial methyl groups in [sc-**1d**]‡.

Overall, the calculation of ΔG_{rel} provides relative strain energies for the transition-state structures [**1b**−**d**]‡ in comparison to [**1a**]‡. Simplistically, we assume that the strain can be attributed to unfavorable transannular interactions caused by pseudoaxial methyl groups (Figure 11). Qualitatively, we find a good agreement between the calculated relative strain energies of [**1b**−**d**]‡ and the experimentally observed relative reactivity: $k_{1a} > k_{1b} \approx k_{1c} > k_{1d}$.

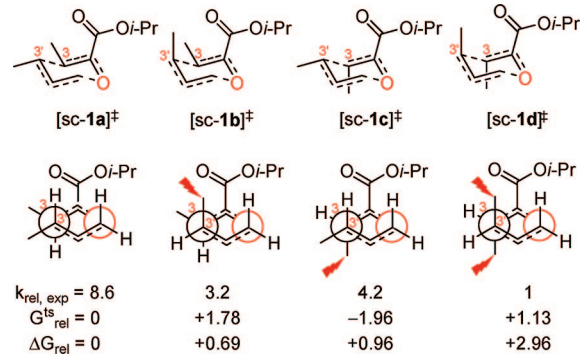

FIGURE 11. Newman projection of [sc-**1a**−**d**]‡, experimentally determined relative rate constant ($k_{rel,exp}$), calculated relative free energies (G^{ts}_{rel}, kcal/mol), and ΔG_{rel} as a measure for the strain energy caused by axial methyl groups.

Conclusions

DFT calculations at the B3LYP/6-31G*+PCM(solvent = 1,2-dichloroethane) level have been used to study the uncatalyzed Gosteli−Claisen rearrangement of the (*E*,*E*)-, (*Z*,*E*)-, (*E*,*Z*)-, and (*Z*,*Z*)-configured allyl vinyl ethers **1a**−**d**. The main conclusions of our work at this level of theory can be summarized as follows:

(1) The conformational flexibility of the C2 ester group was considered by modeling an s-*cis* and s-*trans* pathway for the Gosteli−Claisen rearrangement of **1a**−**d** (Scheme 1). The calculated $\Delta G^{‡}$ values for the s-*cis* and the s-*trans* pathways are comparable (Figures 6−9). The calculated and the experimental $\Delta G^{‡}$ values are in good agreement (Table 1).

(2) The relative stability of the allyl vinyl ethers sc/st-**1a**−**d** is determined by the configuration of the stereogenic C/C double bonds (Table 3, Figure 10). The configuration of the vinyl ether double bond affects the dihedral distortion of the ester carbonyl

relative to the vinyl ether double bond; the allyl vinyl ethers **1c**,**d** featuring a *Z*-configured vinyl ether double bond are characterized by a dihedral angle (ω) closer to planarity.

(3) The Gosteli−Claisen rearrangement of the allyl vinyl ether **1a**−**d** is characterized by a concerted bond reorganization process via a transition-state structure with more bond-breaking than bond-making character (Table 2). The interfragment charge-separation declines by going from the ground to the transition-state; nevertheless, at the same time, the dipole moment increases due to the increasing distance of the allylic and the oxallylic fragment within the transition-state structure.

(4) The relative stability of the chairlike transition-state structures [sc/st-**1a**−**d**]‡ of the Gosteli−Claisen rearrangement is determined by the number and position of destabilizing pseudoaxial methyl groups and the dihedral angel ω (Figure 10). The relative transition-state stability (G^{ts}_{rel}) does not reflect the relative reactivity (k_{rel}) of the corresponding allyl vinyl ethers sc/st-**1a**−**d** (Figure 11).

(5) The relative reactivity (k_{rel}) of the four double bond isomeric allyl vinyl ethers sc/st-**1a**−**d** is attributable to unfavorable transannular interactions (strain) caused by pseudoaxial methyl groups in the corresponding transition-state structures [sc/st-**1a**−**d**]‡ (Figure 11).

The results of our effort provide a foundation for further experimental and computational studies on the catalyzed and uncatalyzed Gosteli−Claisen rearrangement. In particular, our experimental data and computational results should assist in elucidating the mechanistic details of the catalytic cycle of the Lewis acid catalyzed Gosteli−Claisen rearrangement, namely, rate acceleration and stereodifferentiation. The results of a study aimed at this objective will be reported in due course.

Acknowledgment. We acknowledge the Deutsche Forschungsgemeinschaft (HI 628/4) and the itmc of the TU Dortmund for generous support of this work. J.R. thanks Prof. Thomas Strassner and Prof. Gotthard Seifert (both Technische Universität Dresden) for advice and encouragement.

Supporting Information Available: Cartesian coordinates for ground and transition-states, imaginary frequencies, total electronic energies, zero-point vibrational energies of all stationary points of the *s-cis* and *s-trans* pathways. Additional geometric data, energies, and illustrations of all stationary points of the *s-cis* and *s-trans* pathways. This material is available free of charge via the Internet at http://pubs.acs.org.

JO900635K